© 2017. Published by The Company of Biologists Ltd | Journal of Cell Science (2017) 130, 2371-2381 doi:10.1242/jcs.186411

RESEARCH ARTICLE

Caspase-9 has a nonapoptotic function in *Xenopus* embryonic primitive blood formation

Hong Thi Tran[1,*], Mathias Fransen[1,*], Dionysia Dimitrakopoulou[1], Griet Van Imschoot[1,2], Nicolas Willemarck[1] and Kris Vleminckx[1,‡]

ABSTRACT

Caspases constitute a family of cysteine proteases centrally involved in programmed cell death, which is an integral part of normal embryonic and fetal development. However, it has become clear that specific caspases also have functions independent of cell death. In order to identify novel apoptotic and nonapoptotic developmental caspase functions, we designed and transgenically integrated novel fluorescent caspase reporter constructs in developing *Xenopus* embryos and tadpoles. This model organism has an external development, allowing direct and continuous monitoring. These studies uncovered a nonapoptotic role for the initiator caspase-9 in primitive blood formation. Functional experiments further corroborated that caspase-9, but possibly not the executioners caspase-3 and caspase-7, are required for primitive erythropoiesis in the early embryo. These data reveal a novel nonapoptotic function for the initiator caspase-9 and, for the first time, implicate nonapoptotic caspase activity in primitive blood formation.

KEY WORDS: Caspase, Apoptosis, Erythropoiesis, Differentiation, *Xenopus*

INTRODUCTION

Cell death is a fundamental aspect of development of almost all multicellular organisms in which it is essential to control tissue homeostasis, to eliminate aged or damaged cells and to shape the embryo (Fuchs and Steller, 2011; Penaloza et al., 2006). The predominant contribution of developmental cell death can be attributed to the process of apoptosis or programmed cell death. Two main evolutionarily conserved protein families are involved in apoptosis, namely members of the Bcl-2 protein family, which control mitochondrial integrity (Youle and Strasser, 2008), and caspases, which mediate the execution phase of apoptosis (Fuentes-Prior and Salvesen, 2004). However, a paradigm shift has occurred as it became clear that proteins involved in the induction of apoptosis or apoptotic dismantling of cells also exhibit cell death-unrelated functions (Galluzzi et al., 2012). Growing evidence implicates the cell death machinery as a vital component of the differentiation program (Fernando and Megeney, 2007). Indeed, several caspases are shown to be indispensable for cell maintenance and differentiation processes of diverse cell types (Feinstein-Rotkopf and Arama, 2009; Lamkanfi et al., 2007). This is best documented for the executioner caspase-3 (casp3), which aside from its central role in programmed cell death, also appears to be involved in the terminal differentiation of lens fiber cells and keratinocytes (Weber and Menko, 2005; Weil et al., 1999; Wride et al., 1999). In addition, nonapoptotic casp3 signaling seems to be required for the rather early stages of embryonic stem cell, myoblast, monocyte, erythroblast, osteoblast and osteoclast differentiation (Fernando et al., 2002; Fujita et al., 2008; Miura et al., 2004; Sordet et al., 2002; Szymczyk et al., 2006; Zermati et al., 2001). The initiator caspase-9 (casp9) is involved in at least some of these processes, and indicates the importance of the highly conserved mitochondrial death effectors in cell death-unrelated functions (Fujita et al., 2008; Galluzzi et al., 2008; Murray et al., 2008). It can be expected that caspases are involved in additional processes during organogenesis and tissue formation, both in the adult and in the embryo.

Here, we describe the development of a sensitive and dynamic fluorescent reporter system to detect the spatio-temporal pattern of caspase activation in transgenic *Xenopus* embryos. With the help of this reporter system we uncover a novel nonapoptotic role for casp9 activation in the formation of primitive blood cells in *Xenopus* embryos. The observed casp9 activity in the ventral blood island (VBI) turns out to be independent of the activity of the downstream effectors casp3 and caspase-7 (casp7). Loss-of-function experiments combined with rescue studies show that casp9 is specifically required for the proper expression of erythroid markers, uncovering an essential role in primitive erythropoiesis.

RESULTS

Basic design of the reporter system

We designed a caspase-reporting system based on the transcriptional induction of the eGFP gene. An exogenous transcription factor is fused via a tetrapeptide sequence to the extracellular and transmembrane domains of the interleukin 2 receptor (IL2R). The tetrapeptide can be recognized and cleaved by specific caspases, which frees the GAL4 transcription factor and allows its translocation to the nucleus, where it induces the eGFP reporter under control of the GAL4 upstream activating sequences (UAS) (Fig. 1A). GAL4-based binary systems controlling transgene expression have been used successfully in different organisms, including *Drosophila*, zebrafish and *Xenopus* (Fischer et al., 1988; Grabher and Wittbrodt, 2004; Halpern et al., 2008; Xu et al., 1993). However, since the GAL4 transactivation domain is a potential caspase substrate (van Criekinge et al., 1999), it was exchanged for that of the *Herpes simplex* virus *VP16* gene, which is insensitive to caspase cleavage (van Criekinge et al., 1999). Note that the GAL4 UAS is not activated by any transcription factor of any organism other than yeast (Brand and Perrimon, 1993).

We were primarily interested in the activity of the executioners casp3 and casp7, and the initiator casp9. Hence, we introduced

[1]Department of Biomedical Molecular Biology, Ghent University, B-9052 Ghent, Belgium. [2]VIB-UGent Center for Inflammation Research, B-9052 Ghent, Belgium.
*These authors contributed equally to this work

‡Author for correspondence (kris.vleminckx@irc.UGent.be)

K.V., 0000-0002-9666-4105

Received 18 January 2016; Accepted 30 May 2017

Journal of Cell Science (2017) 130, 2371-2381 doi:10.1242/jcs.186411

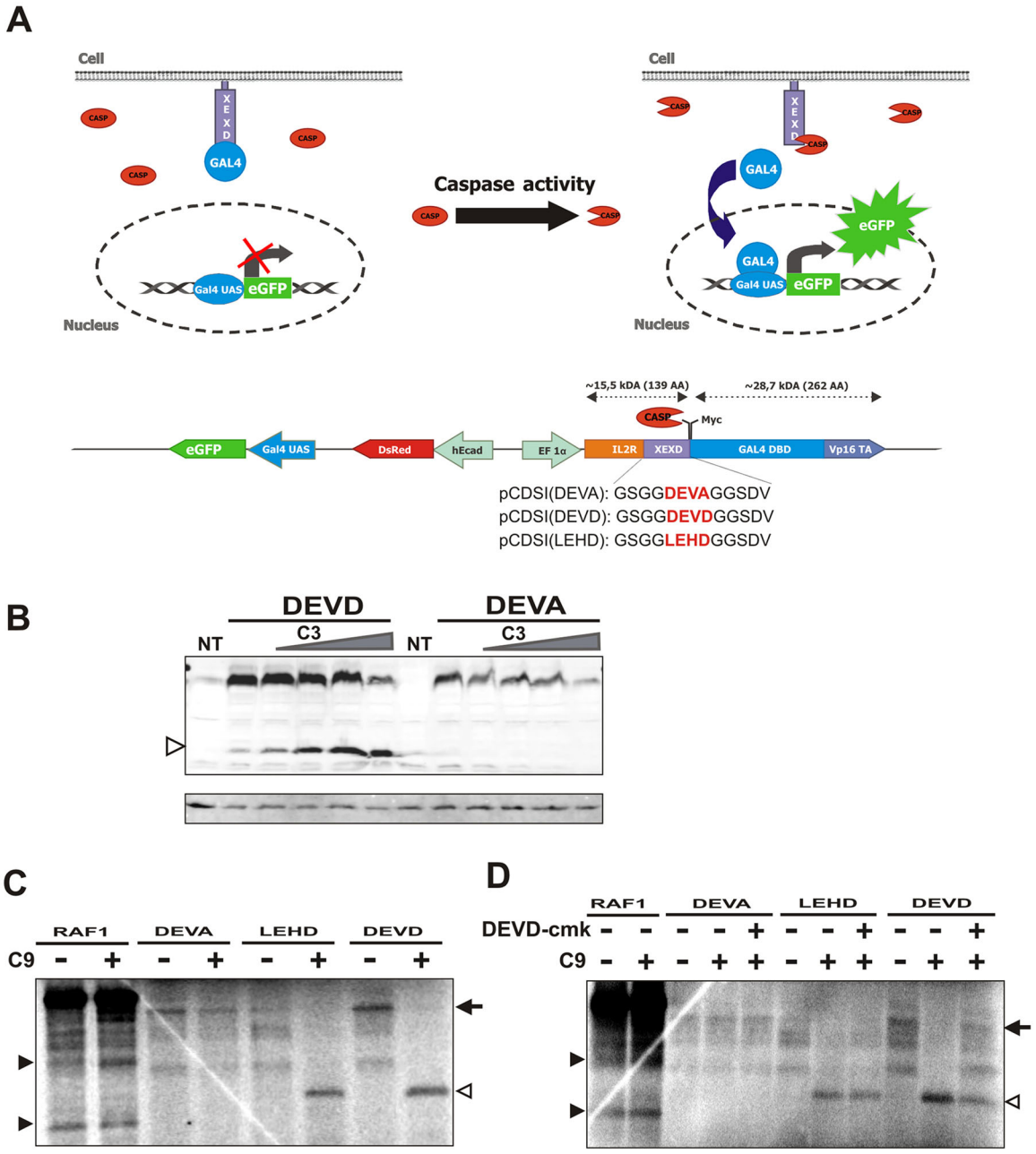

Fig. 1. Design and characterization of the caspase reporter constructs. (A) Schematic representation of the caspase reporter constructs. The GAL4VP16 transcription factor is anchored in the membrane by the extracellular and transmembrane domain of IL2R. Activated caspases cleave their recognition site, freeing the chimeric GAL4VP16 transcription factor, which can then translocate to the nucleus, where it initiates the transcription of the eGFP reporter gene. A general lay-out of the three designed reporter systems with their distinct DNA and AA sequences is shown. (B) Anti-Myc tag western blot analysis of reporter cleavage products in 293t HEK cells cotransfected with mouse casp3. The DEVD reporter, but not the DEVA control reporter, was found to be sensitive to the exogenous casp3 (arrowhead). The DNA coding for the distinct reporter constructs (200 ng) was combined with a DNA gradient (50 ng, 100 ng, 150 ng, 250 ng) coding for casp3. (C) The LEHD reporter system can be proteolytically cleaved by exogenous mouse casp9 in a TNT assay. The three reporter systems were *in vitro* transcribed and translated and subsequently exposed to recombinant mouse casp9 proteins. Raf-1 protein was used as a positive control for cleavage with casp9 (black arrowheads). Both the LEHD and the DEVD constructs are cleaved by casp9 resulting in a 30 kDa fragment (open arrowhead). (D) The addition of the casp3 inhibitor DEVD-cmk (10 µM) prevented the cleavage of the DEVD construct, but not the LEHD construct (open arrowhead), suggesting that the observed cleavage of DEVD by casp9 in C is a result of the casp9-mediated activation of casp3 present in the lysate as an inactive procaspase. The DEVA reporter is insensitive to recombinant casp9. Arrows indicate the uncleaved fragments (~70 kDa). hEcad, human CDH1 promoter; EF1α, *Xenopus* EF1α promoter; IL2R, transmembrane region of the IL2R gene; GAL4 DBD, GAL4 DNA-binding domain; Vp16 TA, transactivation domain of the *Herpes simplex* VP16 gene.

the tetrapeptides DEVD, as a putative substrate for casp3 and casp7, and LEHD, as a putative substrate for casp9. We also designed a DEVA-containing reporter system that lacks the defining aspartate residue located adjacent to the actual cleavage site in the recognition motif. Constructs based on the DEVA tetrapeptide served as a control for nonspecific proteolytic cleavage, and hence nonspecific activation, of the system (McStay et al., 2008).

Journal of Cell Science (2017) 130, 2371-2381 doi:10.1242/jcs.186411

The reporter systems respond to exogenous caspases *in vitro*

Before implementing the reporter systems in living animals, they were validated *in vitro*. The DEVD and LEHD reporters and the DEVA control construct were transiently transfected in 293T cells with or without a concentration gradient of mouse casp3, casp7 or casp9 plasmids. Lysates were prepared 24 h after transfection and immunoblotted for the GAL4VP16 transcription factor. An uncleaved fragment of 70 kDa and a cleaved fragment of ∼30 kDa were detected in cells transfected with the DEVD reporter system together with casp3 (Fig. 1B). No cleaved fragment was observed in cells cotransfected with the DEVA control construct. Unfortunately, we could not document the response of the LEHD detection systems because transfection of exogenous casp9 caused massive death of 293T cells. Therefore, we produced radioactively labeled protein in a cell-free reticulocyte lysate by a combined transcription and translation (TNT) reaction. Recombinant active casp9 protein was added to the reaction mixture, and cleavage was analyzed by gel electrophoresis and visualized by radiography. Addition of casp9 to the IL2R-LEHD-GAL4VP16 protein generated a 30 kDa protein (Fig. 1C). The control IL2R-DEVA-GAL4VP16 protein was resistant to cleavage by casp9. We noticed cleavage of the IL2R-DEVD-GAL4VP16 protein in lysates treated with casp9 (Fig. 1C). However, this probably represents the activation of endogenous casp3 or casp7 by the recombinant casp9, because adding DEVD-cmk, a casp3 and casp7 inhibitor, to the casp9 reaction hampered this cleavage (Fig. 1D). The TNT data and cell culture experiments show that the DEVD and LEHD reporter constructs are cleaved in the presence of exogenous casp3 or casp9, respectively. Importantly, the DEVA control reporter is resistant to caspase cleavage.

The DEVD reporter detects dynamic and specific regions of caspase activity in developing *Xenopus* embryos and tadpoles

Transgenic *Xenopus laevis* and *Xenopus tropicalis* embryos were generated with the three reporter constructs. Transgenic F0 tadpoles could be easily selected due to the expression of the *DsRed* gene, which is present as a marker on all constructs. In early tadpoles expressing the DEVD reporter, dynamic GFP patterns were detected, especially in the brain and spinal cord (Fig. 2). No GFP signals were visible in tadpoles transgenic for the DEVA control reporter, which could be identified by their expression of DsRed (Fig. S1). In total, 14 transgenic *X. laevis* and 12 transgenic *X. tropicalis* embryos were generated with varying levels of reporter gene expression, most likely reflecting copy number variation. Germline transmission of the transgene was obtained in four founder animals (Table S1).

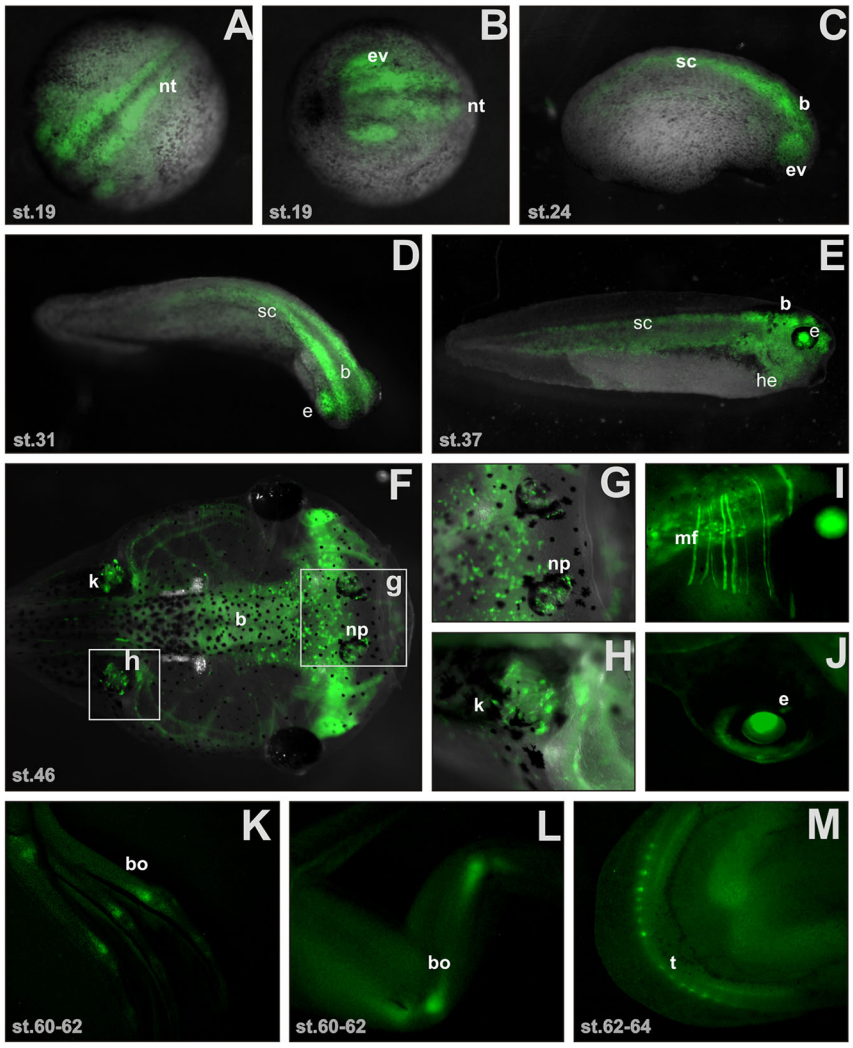

Fig. 2. Transgenic embryos and larvae carrying the DEVD reporter show dynamic spatio-temporal GFP expression patterns during their development. (A) Dorsal and (B) anterior view of a stage 18–19 *X. tropicalis* embryo at neural fold stage. GFP expression emerges in defined stripes on each side of the dorsal midline, which are most intense in the future brain region as well as in the anterior patches corresponding to the eye vesicle. (C) Similar patterns are visible at stage 24 of a *X. tropicalis* tailbud embryo. (D–J) A dynamic and diversified GFP expression signal is observed in reporter embryos as development proceeds. Particularly high expression levels were observed in the developing neural tissues. (F) Stage 46 *X. laevis* tadpoles show GFP positivity in kidney cells (closer view in H), the brain, nasal pits (closer view in G) and muscle fibers (I). (J) The lens was still GFP positive. (K–L) Around metamorphosis (*X. laevis*, stages 60–64), GFP is expressed in the growth zones of the long bones. (M) The teeth and some cranial structures, including the skull and the jawbone, were also GFP positive. b, brain; bo, bone; e, eye; ev, eye vesicle; he, heart; k, kidney cells; mf, muscle fibers; np, nasal pits; nt, neural tube; sc, spinal cord; t, teeth.

Journal of Cell Science (2017) 130, 2371-2381 doi:10.1242/jcs.186411

The spatio-temporal GFP pattern was further documented in living embryos, tadpoles and post-metamorphic transgenic frogs expressing the DEVD reporter (Fig. 2). Similar patterns were observed in *X. laevis* and *X. tropicalis* lines. Interestingly, the GFP patterns observed with the DEVD reporter embryos were strikingly similar to the terminal deoxynucleotidyl transferase-mediated dUTP nick end labeling (TUNEL)-positive regions described by Hensey and Gautier (1998) (see also Fig. S2) and were detected throughout the developing early tadpole. This is consistent with the rather ubiquitous distribution pattern of casp3 and casp7 transcripts during early development (Fig. S3). In the DEVD reporter, starting from the neural fold stage (Nieuwkoop stages 14–19), an intense GFP signal emerged in defined stripes flanking the dorsal midline (Fig. 2A-C). The signal faded out posteriorly and was most intense in the future brain region and the optic vesicle. These patterns were visible throughout the neurula stages. At tailbud and early tadpole stage 37, the GFP signal was present throughout the developing central nervous system, including all areas of the brain, the retina and the spinal cord (Fig. 2D,E). During late tadpole stages 46, the signal was also evident in sensory organs, such as the nasal pits and the otic vesicle. The developing kidneys were also positive, as were individual muscle fibers (Fig. 2F–J; Fig. S4A). Before and during metamorphosis (stage 58–63), GFP was expressed in the maturing bones of the legs, especially near the growth zone of the long bones (Fig. 2K,L), where hypertrophic chondrocytes die by apoptosis and are replaced by differentiating osteoblasts (Xing and Boyce, 2005). The teeth and some cranial structures, including the skull and the jawbone, were also GFP positive (Fig. 2M). Contrary to our expectations, we could not detect any GFP signal during tail regression even though this process involves apoptosis and caspase activation (Rowe et al., 2005). The signals in the developing retina were examined in greater detail in cryosections showing individual GFP-positive cells in all retinal layers, including the photoreceptors (Fig. 3). Interestingly, GFP expression was also detected in cells contributing to the lens as well as in individual myocytes (Fig. 3; Fig. S4A). In summary, the DEVD reporter system shows dynamic spatio-temporal patterns of GFP expression in regions in which apoptotic cell death is known to occur, and in cells associated with cell death-independent caspase activity.

In vivo validation of the DEVD reporter system

To correlate the observed dynamic spatio-temporal GFP patterns in the DEVD reporter with embryonic cell death processes, we performed TUNEL staining on cryosections of transgenic embryos. We focused our analysis on the developing retina, where developmental cell death is well documented (Valenciano et al., 2009). Individual retinal cells in which GFP colocalizes with TUNEL were clearly detectable (arrowheads in Fig. 4A). Several GFP-positive cells did not show TUNEL staining, which can be expected because TUNEL is a late marker for cell death, detecting DNA strand breaks. Because of the interval between caspase activation and DNA cleavage, we postulate that the reporter system detects earlier events in the cell death process. Evidently, caspase activation events unrelated to apoptosis could also explain this incomplete colocalization.

In addition to TUNEL assays, we also performed immunostaining against active casp3, revealing partial overlap between GFP-positive cells and active casp3 cells (Fig. 4B). Yet again, many GFP-positive cells were not stained with the anti-casp3 antibody, which we suspect to be caused by the activity of other caspases activating the reporter, possibly casp7. Furthermore, some active casp3 cells did not show GFP expression. Again, this is likely inherent to the system since there is a considerable time interval between the actual proteolytic event and the full expression and maturation of the GFP protein in our system. In summary, our transgenic DEVD reporter system detects apoptotic cell death, but not the cells and tissues in which rapid cell death occurs.

The DEVD reporter system reports activity of casp3 and casp7

To assess the specificity of our DEVD reporter system in an *in vivo* context, we used morpholinos to specifically knockdown the expression of casp3 and casp7. Fertilized eggs were injected with the translation-blocking morpholinos targeting casp3 ($C3MO^{ATG}$) and casp7 ($C7MO^{ATG}$), either alone or in combination (Fig. S5). At stages 18–20, lysates were made and subjected to a DEVD-linked coumarin-based fluorescent compound (AMC). Injection of 40 ng of either morpholino resulted in little or no decrease in DEVDase activity (Fig. S6). However, combining the two morpholinos, each at a dose of 10 ng, reduced DEVDase activity by 50%. This synergistic response demonstrates the redundancy between the two caspases.

Next, we injected the combined morpholinos into embryos transgenic for the DEVD reporter system. We targeted the morpholinos unilaterally at the two-cell stage, together with a fluorescent tracer. The uninjected half of the embryo served as an internal control. The targeted knockdown of casp3 and casp7 almost completely abolished GFP expression at the injected site in stage 28

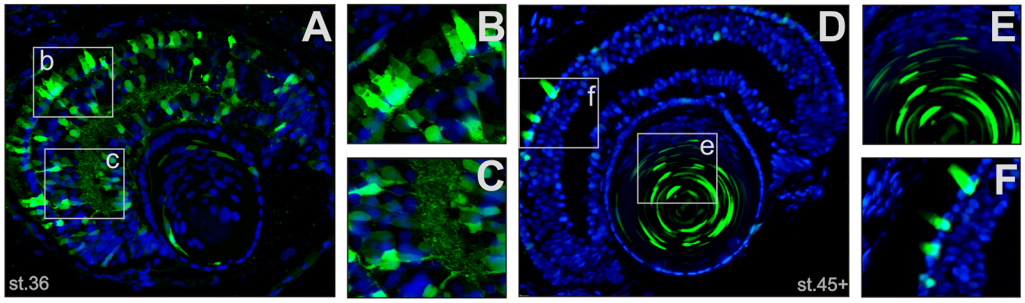

Fig. 3. Highly dynamic caspase activity during eye development. (A–F) Cryosections of the eyes in DEVD reporter *X. laevis* tadpoles at (A-C) stage 36 and (D–F) stage 45+. Nuclei are counterstained with DAPI. (A–C) A DEVD transgenic embryo at stage 36 showed consistent GFP signals in all retinal layers including the ganglion cell layer, the inner nuclear layer and the outer nuclear layer. At this stage, nuclei are still present in the differentiating lens fiber cells. (B) Higher magnification view of the GFP-positive photoreceptors in the box labeled 'b' in A. (C) Higher magnification view of the GFP-positive neuronal network between the different retinal layers in the box labeled 'c' in A. (D,E) GFP is expressed in the enucleated lens fiber cells of stage 45+ embryos (a higher magnification view of the box labeled 'e' is shown in E). A few GFP-positive cells were still observed in the fully developed retina (i.e. photoreceptor layer) (a higher magnification view of the box labeled 'f' is shown in F.

Journal of Cell Science (2017) 130, 2371-2381 doi:10.1242/jcs.186411

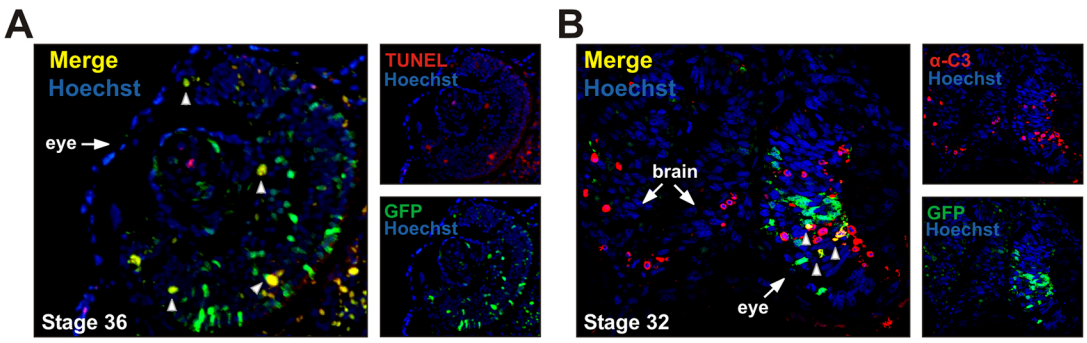

Fig. 4. DEVD reporter activity colocalizes with TUNEL and active casp3 staining. Confocal images of cryosectioned eyes isolated at stages (A) 36 and (B) 32, when massive cell death is occurring in the developing retina (*X. tropicalis*). Arrowheads indicate GFP-positive retinal cells colocalizing with TUNEL-positive cells (A) or active casp3 (B) during retinogenesis. Arrows indicate the eye and the brain on the sections.

embryos (Fig. S6). No changes in GFP expression were observed upon injection of a control morpholino (CoMO) at the same concentration. Hence, the GFP signals obtained in the DEVD reporter line were specific for the activities of casp3 and casp7.

The LEHD reporter system is activated in the VBI

In addition to the DEVD reporter, we also generated transgenic *X. laevis* and *X. tropicalis* with the LEHD reporter system. Of note, despite several attempts, we were unable to establish a transgenic line with this reporter due to lack of germline transmission, for unknown reasons. Therefore, all analyses were performed on F0 animals (*X. laevis* and *X. tropicalis*) (Table S1). Overall, the GFP patterns in embryos and tadpoles showed substantial resemblance to the DEVD reporter, particularly in the regions of the brain, spinal cord and eye (Fig. 5). However, we detected strong GFP expression in the ventral zone of embryos from stage 32 onwards. Interestingly, GFP signals were never detected in this particular region of DEVD reporter animals. This ventral GFP-positive zone corresponds to the VBI. At around stage 28–32, the central domain of this region forms the erythroid lineages of the primitive blood (Ciau-Uitz et al., 2000). At the periphery, vascular lineages are specified. The dynamics of GFP expression in the VBI were monitored by live time-lapse analysis. The first GFP fluorescent signals appeared at ∼stage 30 and the signal intensified until stage 37, when cells started to leave the VBI through the developing vitelline veins, and began to circulate throughout the whole embryo (Fig. S4B). Circulation of GFP-positive blood cells could be seen until tadpole stage 44–45. Microscopic analysis of blood collected at stage 42 showed that most GFP-positive cells had the morphology of erythrocytes (Fig. 5F). Taken together, these data indicate that the initiator casp9 is activated in the VBI, but the executioners casp3 and casp7 are not.

Casp9 activity is required for primitive blood formation

To investigate whether casp9 plays a role in primitive blood formation, we first performed *in situ* hybridization throughout the early developmental stages. Similar to casp3 and casp7, casp9 transcripts were ubiquitously expressed but, unlike the effector caspases, they were enriched in the VBI (Fig. 6). Next, we designed a translation-blocking morpholino (C9MO^{atg1}). The efficiency of this morpholino was evaluated by coinjecting a Myc-tagged *X. tropicalis* casp9 transcript containing the morpholino targeting sequence. Western blot analysis showed efficient depletion of the tagged caspase (Fig. S5A). As casp9 expression is not restricted to the VBI, general casp9 depletion affected the overall morphology of the embryo. Hence, we targeted the region of the embryo that contributes to the VBI, which in *Xenopus* has a dual origin. The anterior part of the VBI (aVBI) is derived from the dorsal mesoderm and can be traced back to the CD1 blastomeres in the 16-cell stage embryo. By contrast, the posterior compartment of the VBI (pVBI)

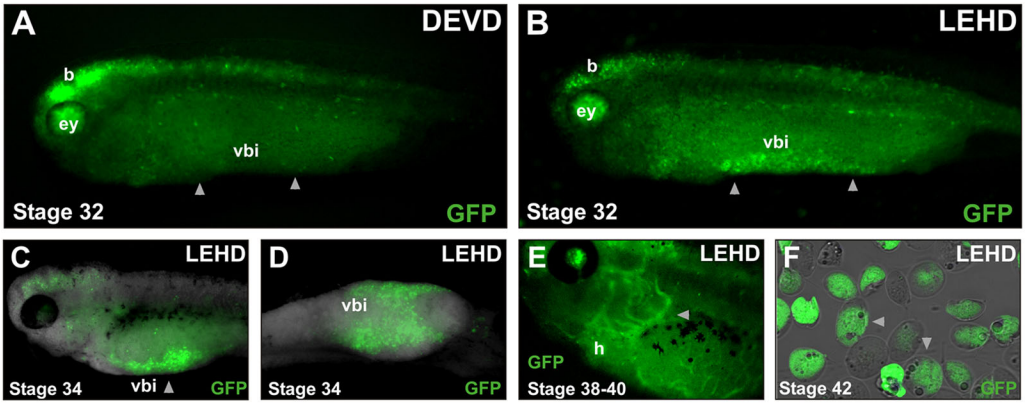

Fig. 5. Activation of the LEHD reporter in the VBI. (A,B) Comparison between the transgenic DEVD and LEHD reporter embryos (*X. tropicalis*) revealed overlapping GFP-positive regions, such as the brain and eye. However, only the LEHD embryos had GFP expression in the VBI, where the primitive blood is formed (arrowheads). (C–D) As development continued, the GFP signal in the VBI intensified and localized in the typical outline of the VBI (ventral view in D). (E) At stage 38–40, GFP-positive cells entered the blood circulation via the vitteline veins. Circulating GFP-expressing blood cells could be detected throughout the embryo (arrowhead). (F) Individual GFP-expressing erythrocytes collected and imaged at stage 42.

Journal of Cell Science (2017) 130, 2371-2381 doi:10.1242/jcs.186411

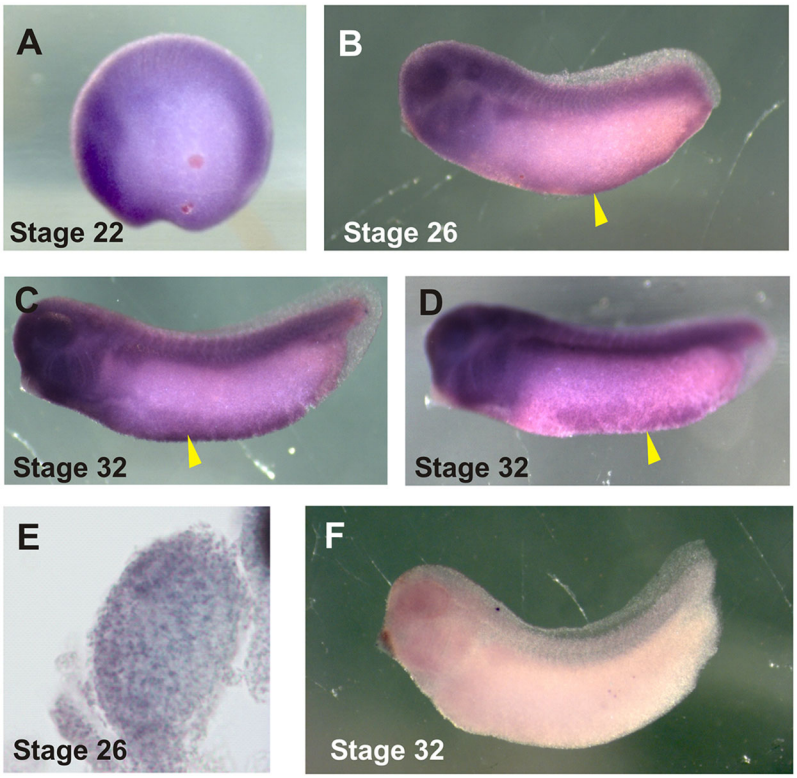

Fig. 6. Casp9 is ubiquitously expressed in early tadpole stages and is slightly enriched in the VBI. (A–D) Expression of *casp9* mRNA at Nieuwkoop stages 22, 26 and 32, as revealed by WISH. Expression is ubiquitous but enriched in some tissues, including the VBI (arrowhead). D shows the same embryo as in C, but in a tilted ventro-lateral view to better expose the VBI. (E) *Casp9* mRNA expression in a vibratome section of the eye vesicle. (F) Control using a sense casp9 probe.

originates in the ventral-most mesoderm and can be targeted by injecting the CD4 blastomeres (Ciau-Uitz et al., 2000). Injecting C9MO^{atg1} in CD4 blastomeres resulted in reduction or loss of the erythroid marker genes *gata1* and αT3 globin (also known as *hba3*) in the pVBI (Fig. 7A). By contrast, injecting a standard morpholino (CoMO) at the same dose only had a minor effect on the expression of these two markers. A significant reduction of αT3 globin transcripts was also observed in an independent experiment upon casp9 knockdown using quantitative RT-PCR (QRT-PCR) (Fig. 7E).

To confirm the specificity of the observed reduction of the primitive blood markers, we designed another translation-blocking morpholino (C9MO^{atg2}) and a splicing morpholino (C9MO^{E2I2}). The second translation-blocking morpholino was directed to the 5′-UTR region of the *X. tropicalis casp9* mRNA. The splicing morpholino was directed against the boundary of exon 2 and intron 2 and its efficacy was monitored by RT-PCR. This analysis showed a reduction of the wild-type *casp9* transcript due to intron retention (Fig. S5B). Targeting these morpholinos to the CD4 blastomeres resulted once more in severe reduction in the expression of the erythroid marker gene αT3 globin (Fig. S7). Consistent depletion of this primitive blood marker by using three different morpholinos confirmed the specificity of our knockdown for embryonic blood formation.

As a final control, we performed a rescue experiment in which we coinjected C9MO^{atg1} with synthetic *X. laevis casp9* mRNA. This transcript has four mismatches in the target sequence of the C9MO^{atg1}. Accordingly, casp9 protein levels obtained from this RNA were not reduced by the C9MO^{atg1}, which makes it ideal for rescue experiments (Fig. S5A). Coinjection of C9MO^{atg1} with the *X. laevis casp9* RNA reduced the percentage of embryos with reduced expression of the T3 globin marker from 78% (n=43) to 34% (n=51) (Fig. 7C,D). Coinjection of *X. laevis casp9* RNA also restored T3 globin marker gene expression in a quantitative RT-PCR experiment (Fig. 7E). In conclusion, the activation pattern and the functional data show that casp9 activity is needed for the formation of primitive erythrocytes during *Xenopus* development.

Depletion of casp3 and casp7 does not interfere with primitive erythropoiesis

Because the DEVD reporter was not activated in the VBI and no TUNEL staining had been found in the VBI (Fig. S2), we wanted to determine whether the activity of casp9 in the VBI is independent of the activation of the executioners casp3 and casp7. Morpholinos depleting the two caspases were targeted to the pVBI, and erythroid markers were analyzed. In contrast to depletion of casp9, codepletion of casp3 and casp7 in the posterior VBI had only a mild or no effect on the expression of erythroid marker genes (Fig. 7A,B,E). This further indicates that the role of casp9 in the process of primitive blood formation is a nonapoptotic event, and is independent of the two downstream executioners casp3 and casp7.

DISCUSSION

Here, we describe a novel transgenic system to detect specific caspase-activity during *Xenopus* development. Transgenic implementation of the constructs in *Xenopus* embryos documented unique and dynamic spatio-temporal patterns of GFP expression, which corresponded to the TUNEL-positive regions described by Hensey and Gautier (1998), and revealed previously documented developmental apoptotic processes (e.g. during retina formation and neurogenesis in the brain) (Hensey and Gautier, 1998; Vecino et al., 2004). Although several methods are available for real-time imaging of caspase activity for cell culture or *ex vivo* experiments, the implementation of methods for whole organisms remains a challenge. Noninvasive reporter systems have been described that monitor real-time caspase activation in living cells and oocytes *in vitro* (Luo et al., 2001; Wu et al., 2006), as well as in whole organisms, such as yeast, the fly, plants and mice (Bardet

Journal of Cell Science (2017) 130, 2371-2381 doi:10.1242/jcs.186411

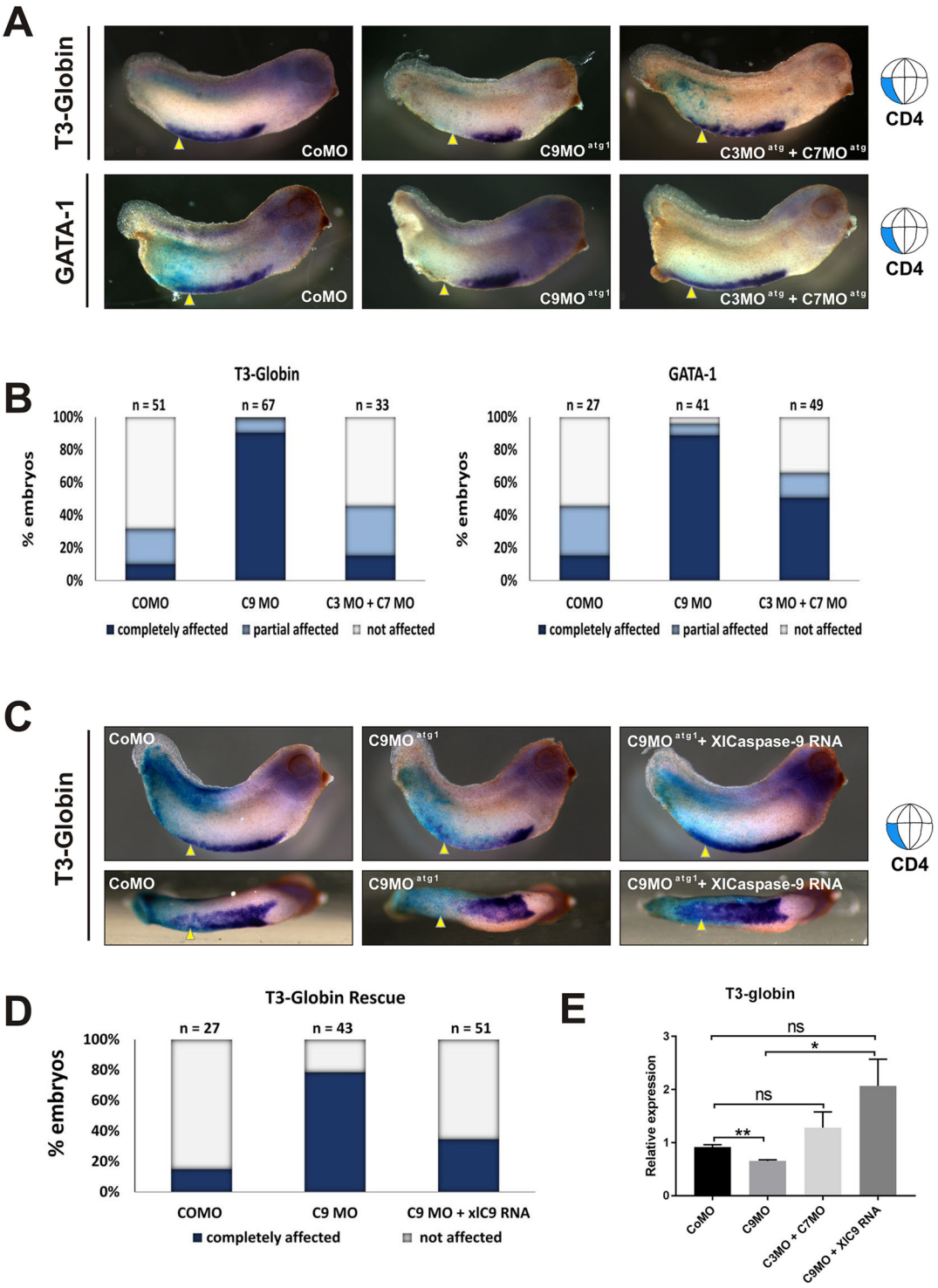

Fig. 7. Knockdown of casp9 depletes the expression of early blood marker genes. (A) *X. tropicalis* embryos were injected in two CD4 blastomeres at 16-cell stage with 2.5 ng C9MO^{atg1}, 4 ng CoMO or a combination of 2 ng C3MO^{atg} and 2 ng C7MO^{atg} in each blastomere. *β-Gal* RNA (10 pg) was coinjected as lineage tracer. WISH analysis of T3 globin and *gata1* expression in the posterior part of the VBI is shown. Both T3 globin and *gata1* expression were affected upon depletion of casp9, but not upon the combined depletion of casp3 and casp7. (B) Graphs representing the percentage of embryos injected in CD4 blastomeres at 16-cell stage, exposing the defects in marker expression. The embryos were scored using the phenotype in A as a reference (based on six independent experiments). (C) Depletion of T3 globin expression could be rescued by *X. laevis casp9* RNA. *X. tropicalis* embryos were injected in two CD4 blastomeres at 16-cell stage with 2.5 ng CoMO, 2.5 ng C9MO^{atg1} or 2.5 ng C9MO^{atg1}, combined with 100 pg *X. laevis casp9* RNA in each blastomere. *β-Gal* RNA was coinjected as a lineage tracer. WISH analysis shows T3 globin expression in the posterior part of the VBI. The overexpression of Xlcasp9 could rescue the defect in T3 globin expression induced by casp9 depletion. (D) The percentages of embryos injected in CD4 blastomeres at 16-cell stage showing the defect in T3 globin marker expression (based on four independent experiments). (E) For quantitative RT-PCR analysis, *X. tropicalis* embryos were injected in two CD4 blastomeres at 16-cell stage with 4 ng CoMO, 2.5 ng C9MO^{atg1} with or without 100 pg *X. laevis* casp9 RNA, or a combination of 2 ng C3MO^{atg} and 2 ng C7MO^{atg} in each blastomere. RT-PCR analysis of T3 globin expression shows significant reduction upon injection of C9MO^{atg1}, which is rescued upon coinjection of *casp9* RNA. T3 globin expression is not significantly affected in C3/C7 double morphants. The graph shows the combination of three biological replicates. ns, not significant; *P<0.05; **P<0.005 (Student's *t*-test).

Journal of Cell Science (2017) 130, 2371-2381 doi:10.1242/jcs.186411

et al., 2008; Garrod et al., 2012; Hawkins et al., 1999; Johnson et al., 2009; Khanna et al., 2010; Yamaguchi et al., 2011; Zhang et al., 2009). Most of these reporters make use of the fluorescence resonance energy transfer (FRET) technology or a surface plasmon resonance imaging system, in which the fluorescent signal is lost after caspase cleavage (Park et al., 2008). Evidently, FRET systems require complex imaging technology to differentiate between the two wavelengths of the fluorophores, and deal with the presence of a ubiquitous fluorescent signal in the absence of caspase activity. This makes large-scale assessment of caspase activity difficult. In addition, other systems such as those based on nuclear translocation of nuclear localization sequence (NLS)-GFP upon caspase activity (Bardet et al., 2008) may lack sensitivity in larger animals, and hence their use is likely to be restricted to highly transparent tissues or organs. Our transcription factor-based reporter is actually an amplification system, which makes it very sensitive and allows the monitoring of low levels of caspase activity. Moreover, activation of the reporter can be assessed on a regular fluorescence stereomicroscope, allowing the continuous evaluation of developing embryos. Interestingly, a conceptually identical transgenic GAL4-based caspase reporter system was very recently reported in *Drosophila*, where it was also shown to detect nonapoptotic processes in the embryo and the adult (Tang et al., 2015). Evidently, our system has limitations that have to be taken into account when assessing the fluorescent patterns. The system is dependent on transcription, translation and GFP maturation, causing a delay in the occurrence of the fluorescent signal upon caspase activation. A characteristic feature of the apoptotic process is the eventual shut down of the transcription and translation machinery (Saelens et al., 2001). Hence, cells undergoing rapid apoptotic cell death are not able to generate a fluorescent signal. This may explain the absence of reporter activity in the regressing tail. We reason that besides the obvious functions of caspases in cell death, our reporter system is ideal to detect the nonapoptotic functions of the investigated caspases (Feinstein-Rotkopf and Arama, 2009; Lamkanfi et al., 2007).

Interestingly, the LEHD transgenic embryos displayed strong GFP expression in the VBI, an activity not seen with the DEVD reporter. Later in development, these GFP-positive cells started to circulate throughout the vitelline veins and formed the primitive erythrocytes. This observation suggested a novel nonapoptotic function for casp9 in blood formation. Indeed, targeted depletion of casp9 in the VBI affected the expression of early erythroid markers. So far we have not been able to identify the substrates that are cleaved by casp9 and consequently potentiate erythropoiesis. Interestingly, while we fail to see a role for casp3 and casp7 for primitive erythropoiesis in *Xenopus*, casp3 has been shown to play a role in different aspects of blood formation in mammals. During human erythroblast differentiation, casp3 was found to be transiently activated through the mitochondrial pathway, where it cleaves proteins involved in nuclear envelope integrity (e.g. lamin B) and chromatin condensation (e.g. acinus), but spares other potential substrates such as GATA1, which is presumably protected by the interaction with HSP70 (Ribeil et al., 2007; Zermati et al., 2001). Of note, *Xenopus* erythrocytes do not extrude their nucleus. Intriguingly, the role of casp3 in mouse erythropoiesis was found to be restricted to the early phases of proerythroblast differentiation, with no major roles in the nuclear substructure reorganization and nuclear extrusion that characterize the late phases of the process (Krauss et al., 2005). In any case, these data, which are all based on *ex vivo* culture conditions suggest an essential role for casp3 in erythropoiesis, which we cannot immediately reconcile with our *in vivo* data. Not only did we not observe any GFP expression at the VBI in the DEVD transgenic embryos, but we also failed to see a convincing effect on the expression of the erythroid markers after combined depletion of casp3 and casp7. Evidently, a certain degree of restraint is appropriate in our interpretation. We cannot exclude that these observations are caused by very low activity of the executioner caspases, which fails to activate the DEVD reporter during primitive blood formation. In addition, morpholino experiments only induce a (temporary) knockdown of their targets. Low remaining protein levels of casp3 or casp7 may be sufficient to allow blood-forming activity. Our strongest argument against this interpretation is that we have never seen GFP expression in the forming VBI, nor in the circulating blood cells in DEVD reporter tadpoles, despite analysis of several F0 and F1 animals, some with very strong transgene expression. Therefore, we favor the interpretation of evolutionary divergence implying that the role of caspases in blood formation may be dissimilar in mammals and frogs. It is also important to mention that all previous studies on nonapoptotic roles for caspases during blood formation are implicating casp3 in definitive (fetal or adult) erythropoiesis, while our study is specifically on primitive (embryonic) blood formation. To our knowledge, no studies have been published on the involvement of caspases in primitive hematopoiesis and, conversely, we do not present any evidence implicating casp9 in definitive hematopoiesis. Primitive and definitive hematopoiesis have very different origins and characteristics (Palis, 2008).

A remaining question is how activation of the effectors casp3 and casp7 is prevented during erythropoiesis. This may involve a member of the family of inhibitors of apoptosis (IAPs) or the protective role for a potential casp9 substrate. However, there are other protective mechanisms that may act downstream of signaling pathways involved in erythrocyte differentiation, such as the Wnt and/or EPO pathways. For instance, Wnt signaling was demonstrated to be crucial for erythropoiesis, potentially via the induction of pro-survival factors (Tran et al., 2010). Likewise, EPO signaling is obviously correlated with erythropoiesis and preserves the correct differentiation of these cells (Ingley et al., 2004). Extended comprehension of these pathways will broaden our insight on how these 'lethal' caspases are balanced to promote survival and differentiation instead of leading to cell death.

In summary, we designed and evaluated highly efficient and reliable transgenic reporter systems detecting caspase activity in reproducible and dynamic patterns during early and late embryonic development. This system provided us with unique evidence for the involvement of casp9 in primitive blood formation. We report that this novel function of casp9 is a nonapoptotic event which is possibly independent of the two downstream executioners casp3 and casp7. It remains to be seen if casp9 is actually cleaving substrates important for primitive blood formation.

MATERIALS AND METHODS

Plasmid construction

Standard cloning techniques were used to generate the different constructs. A multiple element transgenesis vector was built onto the backbone of pBluescript IISK (Stratagene). The *X. laevis* EF1α promoter and the carp E1b basal promoter preceded by a 14-mer of UAS GAL4-binding sites were isolated from the plasmids EF-GVP and UG described by Köster and Fraser (2001) and kindly provided by these authors. In addition, EF-GVP was used for GAL4VP16 fusion. First, the DEVD sequence was inserted behind the EF1α promotor with *Xma*I and *Nde*I. Next, a synthetic oligo coding for the c-Myc epitope tag EQKLISEEDL was ligated adjacent to the DEVD sequence with *Aat*I and *Nco*I. The transmembranal domain of IL2R was isolated from the pCMV-IL2R construct, which was kindly provided by

Journal of Cell Science (2017) 130, 2371-2381 doi:10.1242/jcs.186411

the Gumbiner laboratory (University of Virginia School of Medicine, Charlottesville, USA) and cloned between the DEVD-Myc sequence and the EF1α promoter with *Sma*I. The GAL4VP16 fusion from EF-GVP was amplified with PCR and placed behind the IL2R-DEVD-Myc sequence with *Bgl*II and *Nco*I. Subsequently, this intermediate construct was combined with the UG construct via *Sac*II ligation. The ubiquitous fluorescent reporter DsRed-Express-1 (Clontech), under control of the minimal human E-cadherin promotor (Denayer et al., 2006), was also inserted into the backbone construct opened with *EcoR*V. This resulted in the plasmid pEF-1α-IL2R-DEVD-Myc-GAL4VP16-pEcad-DsRed-UAS-eGFP, or further called DEVD reporter. To generate the DEVA and LEHD reporter constructs, the DEVD recognition sequence was changed by site-directed mutagenesis (Stratagene). Primers used for the DEVA sequence were 5′-GTCGCTTCCTCCAGCCACCTCATCTCC-3′ and 5′-GGAGATGAGGtGGCTGGAGGAAGCGAC-3′. For LEHD, the primers were 5′-GGGAGCGGAGGACTTGAGCACGATGGAGGAAGC-3′ and 5′-GGGAGCGGAGGACTTGAGCACGATGGAGGAAGC-3′. Furthermore, I-SceI meganuclease restriction sites were added to the reporter constructs, allowing easy isolation of the transgenic fragment. I-SceI restriction sites were isolated from a I-SceI-pBlueSK+ construct (a generous gift from Jochen Wittbrodt, COS Heidelberg, Germany) with an *EcoR*I digest, and ligated in the backbone vectors of the reporter systems with a *Mfe*I digest.

For TNT analysis, the reporter IL2R-XEXX-Myc-GAL4VP16 fragments were picked up with PCR and cloned in the mammalian expression vector pcDNA3 via *Apa*I and *Nhe*I digestion (Life Technologies). *Xlcasp9* and *Xtcasp9* cDNAs were amplified by PCR from *X. laevis* and *X. tropicalis* cDNA batches, and subsequently introduced via TOPO cloning technology (Life Technologies) into the pCR2.1-TOPO vector. Next, the caspase-coding fragments were isolated and ligated in the pCS2-Myc tag vector, which was opened with *Xba*I for the Xlcasp9 sequence and with *EcoR*I for the Xtcasp9 sequence, leading to the expression vectors pCS2-Myc-Xlcasp9 and pCS2-Myc-Xtcasp9, respectively.

Immunostaining on cryosections

Transgenic embryos were fixed in 1% paraformaldehyde for 1 h at room temperature, washed with PBS, embedded in 30% sucrose overnight, and then transferred into a mold with cryoembedding compound. Samples were snap frozen on dry ice and stored at −80°C. Cryosections of 10 µm thickness were prepared on a cryotome at −20°C and embedding compound was washed away with PBS. The sections were directly stained with Hoechst 33342 (1:10,000, Life Technologies) or used for colocalization experiments with active casp3, in which sections were incubated with polyclonal rabbit anti-active caspase-3 (1:2000, ab13847, Abcam) and revealed with anti-rabbit IgG Alexa Fluor 633-conjugated antibody (far red) (Life Technologies). All coverslips were mounted with 1% n-propyl gallate glycerol and imaged with a confocal laser scanning microscope (TCS SP5, Leica).

In vitro TNT

pSV-Sport-Raf-1 [from Cornelis et al. (2005)], LMBP 5264, pCMV-SPORT6-hPARP1 (kind gift from Prof. Peter Vandenabeele, Ghent University, Belgium) and the three reporter constructs described in 'Plasmid Construction', pcDNA3-IL2R-DEVD-GAL4VP16, pcDNA3-IL2R-DEVA-GAL4VP16 and pcDNA3-IL2R-LEHD-GAL4VP16, were used as templates for [^{35}S] methionine (PerkinElmer)-radiolabeled *in vitro* TNT in a rabbit reticulocyte lysate system according to the manufacturer's instructions (Promega). The translated proteins (10 µl) were subsequently incubated for 1.5 h at 37°C in CFS buffer with the recombinant mouse caspases in a total volume of 30 µl. Next, samples were boiled for 10 min after addition of Laemmli buffer and separated by 15% SDS-PAGE. The gel was dried before exposing to a film (Amersham Hyperfilm ECL) for radiography.

Cell culture and transfection assay

293T cells (ATCC) were grown at 37°C in DMEM (Life Technologies) supplemented with 10% fetal calf serum (FCS), 2 mM L-glutamine, 100 U/ml penicillin and 0.1 mg/ml streptomycin, and seeded in six-well plates. Cells were regularly tested for contamination. Transient transfections were performed using FuGENE 6 Transfection Reagent (Roche Applied Science). The expressed mouse caspase constructs were all based on the mammalian pCAGGS expression vector. Cells were lysed after 24 h in NP-40 lysis buffer (0.5% NP-40, 150 mM NaCl, 50 mM Tris pH 7.5 and 2 mM EDTA) supplemented with Complete Protease Inhibitor Cocktail (Roche) and cleared by centrifugation at 4°C. The lysates were then dissolved in Laemmli sample buffer and further analyzed by western blotting.

Western blotting

Antibodies used were polyclonal rabbit anti-Myc IgG (1:2000, 562, Immuno Source) and monoclonal rabbit anti-actin (1:10,000, 69100, MP Biomedicals). Total protein lysates (embryos or cells) were prepared by homogenizing with NP-40 supplemented with protease inhibitors. Following centrifugation, equal amounts of protein were separated by 12% or 15% PAGE, blotted on Immobilon-FL PVDF membrane (Millipore), blocked in Odyssey blocking buffer (LI-COR Biosciences) diluted 1:2 with PBS, and incubated with the required primary antibodies. Secondary antibodies used were IRDye 800CW goat anti-mouse IgG, IRDye 800CW goat anti-rabbit IgG, IRDye 680 goat anti-mouse, IRDye 680 goat anti-rabbit (LI-COR Biosciences). Protein expression was analyzed with an Odyssey CLx Infrared Imaging System (LI-COR Biosciences).

Morpholino design and RNA injections

X. tropicalis embryos were collected from natural mating couples and dejellied in 3% cystein in 1× MMR buffer. Embryos were injected while submerged in 0.1× MMR/6% Ficoll and cultured at 22°C. The following antisense morpholino oligonucleotides were obtained against *X. tropicalis* casp9 (GeneTools): CASP9MO^{atg1}, 5′-GAATGTCCCTGTATTCCGGCT-CCAT-3′; CASP9MO^{atg2}, 5′-CATCCGCTCATCGCTTCCGTACATG-3′; CASP9MO^{EI}, 5′-GACAATGGCAGAAATTTACCTCCGC-3′. As control, a standard morpholino (CoMO) (GeneTools) was used. The morpholinos were dissolved and stored according to the manufacturers' instructions and injected at the doses indicated in the figure legends. The expression constructs pCS2-Myc-Xlcaspase-9 and pCS2-Myc-Xtcaspase-9 were linearized with *Not*I, and *in vitro* synthesis of capped RNA was performed using the SP6 mMESSAGE mMACHINE High Yield Capped RNA Transcription Kit (AM1340, Applied Biosystems). C7MO^{atg} (5′-CTGCTCCTCCATCATTTG CTGAATC-3′) and CASP3MO^{atg} (5′-TACACCATTGTGGGATTCTTCC ATC-3′) were obtained from GeneTools.

Whole-mount *in situ* hybridization and β-galactosidase staining

For whole-mount *in situ* hybridization (WISH), casp3, casp7 and casp9 PCR fragments were amplified from the cDNA of stage 32 *X. tropicalis* tadpoles using the following primer pairs: casp3, 5′-ATTAACCCTCACT-AAAGGATGAATTATGGGAAAGTTGG-3′ and 5′-AATACGACTCAC-TATAGGTCAGGATCTGCATGACTTC-3′; casp7, 5′-ATTAACCCTCA-CTAAAGGATGGTGTACAATATGGAGA-3′ and 5′-AATACGACTCA-CTATAGGTTACTTTAAAAAGTAAAATGC-3′; and casp9, 5′-ATTAA-CCCTCACTAAAGGTTCAGTTTCCAGGAGGAGT-3′ and 5′-AATAC-GACTCACTATAGGAGGGATTTGCTTGTAGGT-3′.

Sense and antisense RNA probes from these cDNAs, as well as probes for GATA1 and αT3 globin, were synthesized from cDNA using digoxygenin as a label (Roche Molecular Biochemicals). Embryos were prepared, hybridized and stained as described (Harland, 1991). For detection, BM Purple was used as a substrate for the alkaline phosphatase. For β-galactosidase (β-gal) staining, the embryos were histochemically stained at 37°C in 1× PBS containing 5 mM $K_3Fe(CN)_6$, 5 mM$K_4Fe(CN)_6$, 2 mM $MgCl_2$ and 1 mg/ml X-gal. The embryos were then washed in 1× PBS, refixed for 1 h in 1× MEMFA (0.1 M Mops pH 7.4, 2 mM EGTA, 1 mM $MgSO_4$, and 3.7% formaldehyde), dehydrated in 100% MeOH, and either stored at −20°C or processed immediately for WISH. Embryos hybridized with the caspase probes were further embedded in 5% low-melting-point agarose (Sigma-Aldrich) and sectioned at 100 µm on a vibratome.

Quantitative RT-PCR

X. tropicalis embryos injected with morpholino and/or synthetic mRNA were lysed at stage 32. Ten embryos were pooled for each sample. Total

RNA was extracted using Aurum Total RNA Fatty and Fibrous Tissue Kit (Bio-Rad) and 1 µg RNA was used for cDNA synthesis (iScript Advanced cDNA Synthesis Kit, Bio-Rad). RT-qPCR was performed in triplicate for each sample using the qPCR SensiFAST SYBR No-ROX Kit (Bioline) on the LightCycler 480 (Roche). The specificity of each amplicon was checked by melting curve analysis. The results were normalized with the housekeeping genes *ODC* and *EF1α*. Statistical analysis was performed using GraphPad Prism software. Primers used for αT3 globin were 5′-ACCCCAAGCTAGTGCAATTG-3′ and 5′-TTGCCTCCGTGGTTTT-GAAG-3′; for ODC, 5′-TACGTCAATGATGGAGTGTATGGA-3′ and 5′-CTCATCTGGTTTGGGTTTCTTTGT-3′; and for EF1α, 5′-GCT-GGAAGCTCTTGACTGCATT-3′ and 5′-CCAATACCGCCAATTTTGT-AGAC-3′.

Transgenesis in *Xenopus*

X. tropicalis frogs were obtained from Nasco (http://www.enasco.com) and *X. laevis* from African Reptile Park, South Africa. Transgenesis was performed as described in Hirsch et al. (2002). Briefly, to induce ovulation in *X. tropicalis* frogs, they were primed with 20 U human chorionic gonadotropin (HCG, Sigma-Aldrich) and 36–48 h later boosted with 120 U. Eggs were harvested by squeezing the frogs 4 h after boosting. Eggs were semi-dejellied with 2% cysteine in low Ca^{2+} 1× MMR (0.1 M NaCl, 2 mM KCl, 0.2 mM $CaCl_2$,1 mM $MgCl_2$, 5 mM HEPES, pH 7.5), washed five times with 1× low Ca^{2+} MMR, then transferred to agarose-coated dishes containing 8% Ficoll in 0.1× low Ca^{2+} MMR for injection. The transgene fragment (200 ng) was mixed with the prepared sperm nuclei and 2 µl oocyte extract, which decondenses the sperm nuclei and facilitates the integration of the transgene. The reaction mixture was back-filled into a capillary needle and injected into the collected eggs at a rate of one sperm per nucleus per second. Normal dividing embryos were selected at the four-cell stage (1.5 h after injection), cultured overnight in 6% Ficoll/0.1× MMR, and transferred to 0.1× MMR without Ficoll. Transgenic embryos were screened for fluorescence signal using a Zeiss fluorescence stereomicroscope. Transgenic founder tadpoles were raised to maturity, and at the age of ∼6 months they were crossed with wild-type Nasco frogs to obtain an F1 generation.

TUNEL staining

Cell apoptosis on sections was assayed using the In Situ Cell Death Detection Kit, TMR red (12 156 792 910, Roche Molecular Biochemicals). Briefly, the sections were refixed, washed and permeabilized on ice. Next, they were incubated with the TUNEL reaction mixture in a humidified chamber for 60 min at 37°C in the dark. After washing with PBS, the nuclei were stained in Hoechst 33342 (1:10,000, H21492, Life Technologies) solution for 15 min. Sections were mounted in 1% n-propyl gallate glycerol and pictured with a confocal laser scanning microscope (TCS SP5, Leica), or an automated upright CellM fluorescence microscope (Olympus BX61). Whole-mount TUNEL staining of *X. tropicalis* embryos was based on the methods described by Hensey and Gautier (1998). In short, the embryos were gradually rehydrated in 1× SSC buffer. They were then incubated in terminal deoxynucleotidyl transferase (TdT) buffer (supplied with the enzyme). Terminal ends were labeled overnight with TdT (10533-065, Invitrogen). The enzyme was then washed away with several EDTA/PBS steps and eventually the embryos were transferred in a 2% blocking buffer. The terminal ends were stained with 1/3000 anti-digoxygenin AP antibody (11-093-274-910, Roche). The next day, the antibody was washed away with several MNT wash steps, and treated with alkaline phosphatase buffer. Staining was performed with Nitro-Blue Tetrazolium (NBT) and bromo-4-chloro-3-indolyl-phosphate (BCIP) (tablets).

Acknowledgements

We thank Dr Howard Fearnhead and members of the Vandenabeele laboratory for critical reading and helpful discussions; Amin Bredan for help with editing the manuscript; and Professor Barry Gumbiner, Professor Peter Vandenabeele, Professor Wittbrodt, Dr Köster and Professor Scott E. Fraser for providing plasmids and recombinant proteins.

Competing interests

The authors declare no competing or financial interests.

Author contributions

Conceptualization: H.T.T., M.F., N.W., K.V.; Methodology: H.T.T., M.F., D.D., N.W., G.V.I., K.V.; Validation: H.T.T., M.F., K.V.; Formal analysis: H.T.T., M.F., N.W., K.V.; Investigation: H.T.T., M.F., D.D., G.V.I.; Data curation: H.T.T., M.F., G.V.I., K.V.; Writing - original draft: M.F., K.V.; Writing - review & editing: H.T.T., K.V.; Visualization: H.T.T.; Supervision: K.V.; Project administration: K.V.; Funding acquisition: K.V.

Funding

This study was supported by Research Foundation – Flanders (G.0D87.16N and AUGE/11/14), the Belgian Science Policy (Interuniversity Attraction Poles, IAP7/07), Ghent University (Concerted Research Actions, BOF15/GOA/011), and the Agency for Innovation by Science and Technology (PhD fellowships to M.F. and N.W.).

Supplementary information

Supplementary information available online at
http://jcs.biologists.org/lookup/doi/10.1242/jcs.186411.supplemental

References

Bardet, P.-L., Kolahgar, G., Mynett, A., Miguel-Aliaga, I., Briscoe, J., Meier, P. and Vincent, J.-P. (2008). A fluorescent reporter of caspase activity for live imaging. *Proc. Natl. Acad. Sci. USA* **105**, 13901-13905.

Brand, A. H. and Perrimon, N. (1993). Targeted gene expression as a means of altering cell fates and generating dominant phenotypes. *Development* **118**, 401-415.

Ciau-Uitz, A., Walmsley, M. and Patient, R. (2000). Distinct origins of adult and embryonic blood in Xenopus. *Cell* **102**, 787-796.

Cornelis, S., Bruynooghe, Y., Van Loo, G., Saelens, X., Vandenabeele, P. and Beyaert, R. (2005). Apoptosis of hematopoietic cells induced by growth factor withdrawal is associated with caspase-9 mediated cleavage of Raf-1. *Oncogene* **24**, 1552-1562.

Denayer, T., Van Roy, F. and Vleminckx, K. (2006). In vivo tracing of canonical Wnt signaling in Xenopus tadpoles by means of an inducible transgenic reporter tool. *FEBS Lett.* **580**, 393-398.

Feinstein-Rotkopf, Y. and Arama, E. (2009). Can't live without them, can live with them: roles of caspases during vital cellular processes. *Apoptosis* **14**, 980-995.

Fernando, P. and Megeney, L. A. (2007). Is caspase-dependent apoptosis only cell differentiation taken to the extreme? *FASEB J.* **21**, 8-17.

Fernando, P., Kelly, J. F., Balazsi, K., Slack, R. S. and Megeney, L. A. (2002). Caspase 3 activity is required for skeletal muscle differentiation. *Proc. Natl. Acad. Sci. USA* **99**, 11025-11030.

Fischer, J. A., Giniger, E., Maniatis, T. and Ptashne, M. (1988). GAL4 activates transcription in Drosophila. *Nature* **332**, 853-856.

Fuchs, Y. and Steller, H. (2011). Programmed cell death in animal development and disease. *Cell* **147**, 742-758.

Fuentes-Prior, P. and Salvesen, G. S. (2004). The protein structures that shape caspase activity, specificity, activation and inhibition. *Biochem. J.* **384**, 201-232.

Fujita, J., Crane, A. M., Souza, M. K., Dejosez, M., Kyba, M., Flavell, R. A., Thomson, J. A. and Zwaka, T. P. (2008). Caspase activity mediates the differentiation of embryonic stem cells. *Cell Stem Cell* **2**, 595-601.

Galluzzi, L., Joza, N., Tasdemir, E., Maiuri, M. C., Hengartner, M., Abrams, J. M., Tavernarakis, N., Penninger, J., Madeo, F. and Kroemer, G. (2008). No death without life: vital functions of apoptotic effectors. *Cell Death Differ.* **15**, 1113-1123.

Galluzzi, L., Kepp, O., Trojel-Hansen, C. and Kroemer, G. (2012). Non-apoptotic functions of apoptosis-regulatory proteins. *EMBO Rep.* **13**, 322-330.

Garrod, K. R., Moreau, H. D., Garcia, Z., Lemaître, F., Bouvier, I., Albert, M. L. and Bousso, P. (2012). Dissecting T cell contraction in vivo using a genetically encoded reporter of apoptosis. *Cell Rep.* **2**, 1438-1447.

Grabher, C. and Wittbrodt, J. (2004). Efficient activation of gene expression using a heat-shock inducible Gal4/Vp16-UAS system in medaka. *BMC Biotechnol.* **4**, 26.

Halpern, M. E., Rhee, J., Goll, M. G., Akitake, C. M., Parsons, M. and Leach, S. D. (2008). Gal4/UAS transgenic tools and their application to zebrafish. *Zebrafish* **5**, 97-110.

Harland, R. M. (1991). In situ hybridization: an improved whole-mount method for Xenopus embryos. *Methods Cell Biol.* **36**, 685-695.

Hawkins, C. J., Wang, S. L. and Hay, B. A. (1999). A cloning method to identify caspases and their regulators in yeast: identification of Drosophila IAP1 as an inhibitor of the Drosophila caspase DCP-1. *Proc. Natl. Acad. Sci. USA* **96**, 2885-2890.

Hensey, C. and Gautier, J. (1998). Programmed cell death during Xenopus development: a spatio-temporal analysis. *Dev. Biol.* **203**, 36-48.

Hirsch, N., Zimmerman, L. B., Gray, J., Chae, J., Curran, K. L., Fisher, M., Ogino, H. and Grainger, R. M. (2002). *Xenopus tropicalis* transgenic lines and their use in the study of embryonic induction. *Dev. Dyn.* **225**, 522-35.

Ingley, E., Tilbrook, P. A. and Klinken, S. P. (2004). New insights into the regulation of erythroid cells. *IUBMB Life* **56**, 177-184.

Johnson, C. E., Freel, C. D. and Kornbluth, S. (2009). Features of programmed cell death in intact Xenopus oocytes and early embryos revealed by near-infrared fluorescence and real-time monitoring. *Cell Death Differ.* **17**, 170-179.
Khanna, D., Hamilton, C. A., Bhojani, M. S., Lee, K. C., Dlugosz, A., Ross, B. D. and Rehemtulla, A. (2010). A transgenic mouse for imaging caspase-dependent apoptosis within the skin. *J. Invest. Dermatol.* **130**, 1797-1806.
Köster, R. W. and Fraser, S. E. (2001). Tracing transgene expression in living zebrafish embryos. *Dev. Biol.* **233**, 329-346.
Krauss, S. W., Lo, A. J., Short, S. A., Koury, M. J., Mohandas, N. and Chasis, J. A. (2005). Nuclear substructure reorganization during late-stage erythropoiesis is selective and does not involve caspase cleavage of major nuclear substructural proteins. *Blood* **106**, 2200-2205.
Lamkanfi, M., Festjens, N., Declercq, W., Vanden Berghe, T. and Vandenabeele, P. (2007). Caspases in cell survival, proliferation and differentiation. *Cell Death Differ.* **14**, 44-55.
Luo, K. Q., Yu, V. C., Pu, Y. and Chang, D. C. (2001). Application of the fluorescence resonance energy transfer method for studying the dynamics of caspase-3 activation during UV-induced apoptosis in living HeLa cells. *Biochem. Biophys. Res. Commun.* **283**, 1054-1060.
McStay, G. P., Salvesen, G. S. and Green, D. R. (2008). Overlapping cleavage motif selectivity of caspases: implications for analysis of apoptotic pathways. *Cell Death Differ.* **15**, 322-331.
Miura, M., Chen, X.-D., Allen, M. R., Bi, Y., Gronthos, S., Seo, B.-M., Lakhani, S., Flavell, R. A., Feng, X.-H., Robey, P. G. et al. (2004). A crucial role of caspase-3 in osteogenic differentiation of bone marrow stromal stem cells. *J. Clin. Invest.* **114**, 1704-1713.
Murray, T. V., McMahon, J. M., Howley, B. A., Stanley, A., Ritter, T., Mohr, A., Zwacka, R. and Fearnhead, H. O. (2008). A non-apoptotic role for caspase-9 in muscle differentiation. *J. Cell Sci.* **121**, 3786-3793.
Palis, J. (2008). Ontogeny of erythropoiesis. *Curr. Opin Hematol.* **15**, 155-161.
Park, K., Ahn, J., Yi, S. Y., Kim, M. and Chung, B. H. (2008). SPR imaging-based monitoring of caspase-3 activation. *Biochem. Biophys. Res. Commun.* **368**, 684-689.
Penaloza, C., Lin, L., Lockshin, R. A. and Zakeri, Z. (2006). Cell death in development: shaping the embryo. *Histochem. Cell Biol.* **126**, 149-158.
Ribeil, J.-A., Zermati, Y., Vandekerckhove, J., Cathelin, S., Kersual, J., Dussiot, M., Coulon, S., Moura, I. C., Zeuner, A., Kirkegaard-Sørensen, T. et al. (2007). Hsp70 regulates erythropoiesis by preventing caspase-3-mediated cleavage of GATA-1. *Nature* **445**, 102-105.
Rowe, I., Le Blay, K., Du Pasquier, D., Palmier, K., Levi, G., Demeneix, B. and Coen, L. (2005). Apoptosis of tail muscle during amphibian metamorphosis involves a caspase 9-dependent mechanism. *Dev. Dyn.* **233**, 76-87.
Saelens, X., Kalai, M. and Vandenabeele, P. (2001). Translation inhibition in apoptosis: caspase-dependent PKR activation and eIF2-alpha phosphorylation. *J. Biol. Chem.* **276**, 41620-41628.
Sordet, O., Rebe, C., Plenchette, S., Zermati, Y., Hermine, O., Vainchenker, W., Garrido, C., Solary, E. and Dubrez-Daloz, L. (2002). Specific involvement of caspases in the differentiation of monocytes into macrophages. *Blood* **100**, 4446-4453.
Szymczyk, K. H., Freeman, T. A., Adams, C. S., Srinivas, V. and Steinbeck, M. J. (2006). Active caspase-3 is required for osteoclast differentiation. *J. Cell. Physiol.* **209**, 836-844.
Tang, H. L., Tang, H. M., Fung, M. C. and Hardwick, J. M. (2015). In vivo CaspaseTracker biosensor system for detecting anastasis and non-apoptotic caspase activity. *Sci. Rep.* **5**, 9015.
Tran, H. T., Sekkali, B., Van Imschoot, G., Janssens, S. and Vleminckx, K. (2010). Wnt/beta-catenin signaling is involved in the induction and maintenance of primitive hematopoiesis in the vertebrate embryo. *Proc. Natl. Acad. Sci. USA* **107**, 16160-16165.
Valenciano, A. I., Boya, P. and de la Rosa, E. J. (2009). Early neural cell death: numbers and cues from the developing neuroretina. *Int. J. Dev. Biol.* **53**, 1515-1528.
van Criekinge, W., Cornelis, S., Van De Craen, M., Vandenabeele, P., Fiers, W. and Beyaert, R. (1999). GAL4 is a substrate for caspases: implications for two-hybrid screening and other GAL4-based assays. *Mol. Cell Biol. Res. Commun.* **1**, 158-161.
Vecino, E., Hernandez, M. and Garcia, M. (2004). Cell death in the developing vertebrate retina. *Int. J. Dev. Biol.* **48**, 965-974.
Weber, G. F. and Menko, A. S. (2005). The canonical intrinsic mitochondrial death pathway has a non-apoptotic role in signaling lens cell differentiation. *J. Biol. Chem.* **280**, 22135-22145.
Weil, M., Raff, M. C. and Braga, V. M. M. (1999). Caspase activation in the terminal differentiation of human epidermal keratinocytes. *Curr. Biol.* **9**, 361-364.
Wride, M. A., Parker, E. and Sanders, E. J. (1999). Members of the bcl-2 and caspase families regulate nuclear degeneration during chick lens fibre differentiation. *Dev. Biol.* **213**, 142-156.
Wu, Y., Xing, D., Luo, S., Tang, Y. and Chen, Q. (2006). Detection of caspase-3 activation in single cells by fluorescence resonance energy transfer during photodynamic therapy induced apoptosis. *Cancer Lett.* **235**, 239-247.
Xing, L. and Boyce, B. F. (2005). Regulation of apoptosis in osteoclasts and osteoblastic cells. *Biochem. Biophys. Res. Commun.* **328**, 709-720.
Xu, L., Schaffner, W. and Rungger, D. (1993). Transcriptional activation by recombinant GAL4-VP16 in the Xenopus oocyte. *Nucleic Acids Res.* **21**, 2775.
Yamaguchi, Y., Shinotsuka, N., Nonomura, K., Takemoto, K., Kuida, K., Yosida, H. and Miura, M. (2011). Live imaging of apoptosis in a novel transgenic mouse highlights its role in neural tube closure. *J. Cell Biol.* **195**, 1047-1060.
Youle, R. J. and Strasser, A. (2008). The BCL-2 protein family: opposing activities that mediate cell death. *Nat. Rev. Mol. Cell Biol.* **9**, 47-59.
Zermati, Y., Garrido, C., Amsellem, S., Fishelson, S., Bouscary, D., Valensi, F., Varet, B., Solary, E. and Hermine, O. (2001). Caspase activation is required for terminal erythroid differentiation. *J. Exp. Med.* **193**, 247-254.
Zhang, L., Xu, Q., Xing, D., Gao, C. and Xiong, H. (2009). Real-time detection of caspase-3-like protease activation in vivo using fluorescence resonance energy transfer during plant programmed cell death induced by ultraviolet C overexposure. *Plant Physiol.* **150**, 1773-1783.